

# Three-dimensional lowest-Landau-level theory applied to $\text{YBa}_2\text{Cu}_3\text{O}_{7-\delta}$ magnetization and specific heat data: Implications for the critical behavior in the $H$ - $T$ plane

Stephen W. Pierson\*

*Department of Physics, Worcester Polytechnic Institute, Worcester, Massachusetts 01609-2280*

Oriol T. Valls

*School of Physics and Astronomy and Minnesota Supercomputer Institute, University of Minnesota, Minneapolis, Minnesota 55455-0149*

Zlatko Tešanović

*Department of Physics and Astronomy, Johns Hopkins University, Baltimore, Maryland 21218*

Michael A. Lindemann

*Department of Physics, Worcester Polytechnic Institute, Worcester, Massachusetts 01609-2280*

(Received 18 February 1997; revised manuscript received 24 October 1997)

We study the applicability of magnetization and specific heat equations derived from a lowest-Landau-level (LLL) calculation, to the high-temperature superconducting (HTSC) materials of the  $\text{YBa}_2\text{Cu}_3\text{O}_{7-\delta}$  (YBCO) family. We find that significant information about these materials can be obtained from this analysis, even though the three-dimensional LLL functions are not quite as successful in describing them as the corresponding two-dimensional functions are in describing data for the more anisotropic HTSC Bi- and Tl-based materials. The results discussed include scaling fits, evidence for the correspondence between the onset of  $H_{c2}$  (or LLL) fluctuations and the flux lattice melting transition, and reasons why three-dimensional (3D)  $XY$  scaling may have less significance than previously believed. We also demonstrate how 3D  $XY$  scaling does not describe the specific heat data of YBCO samples in the critical region. Throughout the paper, the importance of fitting the actual functions to the data, in contradistinction to checking for scaling behavior, is stressed. [S0163-1829(98)06814-3]

## I. INTRODUCTION

The critical behavior of the high-temperature superconductors in finite magnetic fields applied perpendicular to the copper oxide planes has been described by both lowest Landau level (LLL) theory and three-dimensional (3D)  $XY$  theory with varying degrees of success. It is widely expected that 3D  $XY$  behavior should hold at low fields and that LLL should be valid at higher fields. There is however little consensus about what the value of the crossover field should be and how well either of these theories describe resistivity data, magnetization data, or specific heat data.<sup>1-4</sup> One group<sup>5</sup> has claimed that LLL should not be valid for fields less than ten tesla (T) in deoxygenated  $\text{YBa}_2\text{Cu}_3\text{O}_{7-\delta}$  (YBCO) thin films based on conductivity measurements while three of the present authors<sup>6,7</sup> have found it to be valid down to approximately two tesla based on an analysis of specific heat data from YBCO and  $\text{LuBa}_2\text{Cu}_3\text{O}_{7-\delta}$  (LBCO) single crystals. In Ref. 8, 3D LLL scaling was found to work for fields greater than 6 T while 3D  $XY$  was found to work for fields up to 8 T when domain structure effects were accounted for. They also found that 3D  $XY$  scaled data at lower fields for several YBCO class materials roughly collapse. To minimize the problems of background subtraction and normalization, the authors of Ref. 4 worked with field and temperature derivatives of the specific heat. They found that 3D  $XY$  agreed with their data for fields larger than 1 T and that 3D LLL did for fields greater than 6 T if a nonlinear temperature dependence

was allowed for  $H_{c2}(T)$ . The authors of Ref. 9 on the other hand suggest that their data indicates that 3D  $XY$  theory is not valid beyond 0.5 T and conclude that apparently good scaling of the magnetization is not sufficient for proving the validity of the 3D  $XY$  or the LLL theory. Clearly, there is considerable controversy in this field. This is in great part due to the extreme experimental difficulty in trying to determine, for example, the shape of the specific heat peak, which is a small percentage of the total specific heat signal.

In this work, we address one aspect of this problem where theoretical work can be of some help. We do so by considering existing analytical expressions for the scaling functions, which are available from LLL theory. The existence of theoretically calculated scaling functions should be contrasted with the mere idea of scaling. Scaling is simply the statement that a dimensionless form of a quantity, such as the specific heat or magnetization, can be written as *some* function of a certain dimensionless scaling variable. While the scaling variable is known, the function need not be, and typically it is not. Equations (8), (13), and (14) below are examples of scaling statements. Both the scaling variable and the dimensionless form of the particular quantity depend upon the theory (e.g., LLL or  $XY$ ) and upon the dimensionality. It is possible for experimental data to be consistent with different forms of scaling, particularly if the experimental uncertainty is considerable. On the other hand, a theory may predict the specific form of the scaling functions in addition to the scaling variables. These clearly contain much more information than the variables alone and allow detailed

comparison with experiment for all relevant quantities, not only dimensionless ratios. Experiment may rule out a theory if the theory's scaling functions disagree with the experiment, even if the data appears to scale consistently with the scaling variables in that theory. Conversely, detailed agreement of scaling functions with experiment is a much stronger indication of the correctness of a theory than mere agreement in the scaling variables. Unfortunately, only in the case of the LLL scaling are there analytical expressions for the magnetization and specific heat functions [given by Eqs. (1) and (2) below]. The equivalent analysis cannot yet be done for XY theory.

Analytic expressions for the magnetization and specific heat LLL scaling functions for two-dimensional (2D), three-dimensional (3D), and layered systems have been derived<sup>10,11</sup> by using the LLL approximation in the Ginzburg-Landau (GL) formalism. The two-dimensional portion of this work has had striking success in describing the magnetization of the highly anisotropic high-temperature superconducting materials  $\text{Bi}_2\text{Sr}_2\text{CaCu}_2\text{O}_8$  (BSCCO-2212) and the TI-based compounds for magnetic fields applied perpendicular to the copper oxide planes. For example, the two-dimensional (2D) functions<sup>10,11</sup> have a field independent value at a particular temperature  $T^{*12}$  which is also a crossing point for the magnetization curves. Such behavior has been observed in BSCCO-2212 by many authors<sup>13</sup> and furthermore, Wahl and co-workers<sup>14</sup> have not only observed such crossover in their magnetization data from TI-based single crystals but they have also fit the 2D functions of Refs. 10 and 11 to their data finding good agreement.

Little work has been done to fit the theoretical functions to specific heat data on the highly anisotropic HTSC materials. Kobayashi *et al.*<sup>15</sup> are among the few to publish specific heat data<sup>16</sup> for various fields near the critical temperature on such compounds. They scaled their specific heat data from a *c*-axis aligned  $(\text{Bi,Pb})_2\text{Sr}_2\text{Ca}_2\text{Cu}_3\text{O}_x$  bulk sample and compared it to the 2D scaling function of Tešanović and co-workers<sup>10,11</sup> finding reasonable agreement. They also found a crossing point in their magnetization data.

Even less has been done to compare the theoretical expressions and scaling functions to experimental data for the more isotropic YBCO materials. In Ref. 6, an approximation to the 3D LLL specific heat function was compared to scaled specific heat data from various YBCO samples (including a YBCO single crystal from Ref. 1) and a LBCO sample, with satisfactory agreement. Further, in the work of Ref. 4, although a quantitative comparison was not made, one can find qualitative agreement between the scaled temperature derivatives of the specific heat and the second derivative of the 3D magnetization function. [See Eq. (5) and Figs. 6 and 8 of that reference and Fig. 2 of Ref. 17.] Lastly, we are not aware of any work comparing the 3D theoretical magnetization function to magnetization data of YBCO-class materials (although an LLL scaling variable analysis of this data has been performed<sup>4,9</sup>). This can be attributed in part to the complexity<sup>18</sup> of the 3D specific heat and magnetization functions of Ref. 11.

In this paper, we examine the 3D specific heat and magnetization functions of Ref. 11 comparing them to data from YBCO samples. Not only is such a comparison lacking and certainly needed in order to learn more about the validity of

the theory but we will see that it yields valuable insights into other questions about the behavior of the YBCO materials, besides the nature of their fluctuation behavior. For example, we will present evidence for the correspondence between the onset of  $H_{c2}$  (or LLL) fluctuations and flux lattice melting.<sup>19,20</sup> Furthermore, it will also be seen that the 3D XY scaling is so general as to describe "theoretical data" derived using the LLL theory. This exemplifies the importance of knowing the actual scaling function.

Our focus here will not be so much on the validity of LLL scaling for the HTSC materials as on the applicability of the specific expressions and scaling functions from one particular calculation based on a nonperturbative approach to the GL-LLL theory.<sup>10,11</sup> There are two separate issues here. First, there is the question of describing the HTSC's in a GL-LLL formalism, which has already been answered, in our opinion, through the success of LLL scaling. Second, while the expressions we use are of compact form and should be useful for analysis of experiments and phenomenology, they are not mathematically identical to the exact solution of the GL-LLL theory. Therefore, there is a need to address any possible disagreement between theory and experiment arising from the additional approximations involved in the expressions for the scaling functions of Refs. 10,11 relative to the exact answer within the GL-LLL theory. Although this issue is essentially resolved for very anisotropic, "almost" 2D HTSC systems where the 2D LLL scaling functions of Refs. 10,11 are known to be very accurate,<sup>21</sup> it has not been investigated for the relatively isotropic materials of the YBCO class.

In this work, we take advantage of the availability of numerical work on the (quasi) 3D GL-LLL model.<sup>22</sup> The existence of this numerical work for the magnetization will allow us, as we shall see, to determine some of the fitting parameters in a way that it is not constrained with experimental uncertainties involving, for example, the subtraction of "background" terms. We can say that we use these numerical results to "calibrate" certain parameters in the scaling functions. This is very convenient, since the increased complexity of the 3D functions, as opposed to the 2D case, would otherwise make our task much more intricate and the conclusions weaker.

The paper is organized as follows: The theoretical functions calculated from the nonperturbative<sup>10,11</sup> approach to the GL-LLL theory will be set forth and discussed in Sec. II A. In Sec. II B, the "calibration" fits of the numerical 3D magnetization data to the theoretical result [Eq. (1)] are performed, and then fits to actual magnetization data from YBCO samples are done. Then, in Sec. II C, we give a simple explanation of the peculiar behavior of the field dependence of the partial derivative  $\partial M(H,T)/\partial T$  found<sup>23</sup> in YBCO and BSCCO. We show that this behavior is simply explained in terms of the LLL scaling functions. Fits of the theoretical 3D specific heat function [Eq. (2)] to specific heat data from the same materials as in Sec. II B are reported in Sec. II D along with evidence for the coincidence of the flux lattice melting transition and the onset of  $H_{c2}$  fluctuations. Finally, implications of this work for 3D XY scaling and the importance of the scaling functions is demonstrated in Sec. II E followed by a discussion and summary in Sec. III.

## II. THEORETICAL FUNCTIONS AND DATA FITS

### A. Theoretical GL-LLL functions

As mentioned above, the 2D functions of Refs. 10,11 have had considerable success in describing magnetization data from the highly anisotropic HTSC materials. Here, we will focus on the 3D specific heat and magnetization functions since the 2D functions are already examined and the quasi-2D functions are less tractable. The magnetization as a function of applied magnetic field  $H$  and temperature  $T$  is written as Eq. (26) of Ref. 11

$$\begin{aligned} & \frac{4\pi M(H,T)H'_{c2}}{(TH)^{2/3}} \left( \frac{4\sqrt{2}\pi T_{c0}\xi\kappa\phi_0}{k_B H'_{c2}} \right)^{2/3} \\ &= \left( g + \sqrt{g^2 + \frac{\tan^{-1}Q}{\pi U^2}} \right)^{1/3} \\ & \quad \times [GU^2 - U\sqrt{G^2U^2 + 2}]. \end{aligned} \quad (1)$$

The specific heat function can be rewritten (including important subleading terms) by considering<sup>24</sup> the pure 3D limit of the quasi-3D result [Eq. (30) of Ref. 11]:

$$\begin{aligned} \frac{C(H,T)}{C_{MF}(T)} &= \frac{1}{2} \left( 1 - \frac{GU}{\sqrt{G^2U^2 + 2}} \right) \\ & \quad \times \left[ U^2 \frac{dG}{dg} + (\sqrt{G^2U^2 + 2} - GU) \left| \frac{dU}{dG} \right| \right], \end{aligned} \quad (2)$$

where

$$U(G) = 0.818 - 0.110 \times \tanh\left(\frac{G+K}{M}\right), \quad (3)$$

$$G = g + I \left( g + \sqrt{g^2 + \frac{\tan^{-1}Q}{\pi U^2}} \right), \quad (4)$$

$I = (Q - \tan^{-1}Q)/[2\tan^{-1}Q]$ , and it can be shown that

$$\frac{dG}{dg} = \frac{I g + (1+I)\sqrt{g^2 + \tan^{-1}Q/[\pi U^2]}}{\sqrt{g^2 + \tan^{-1}Q/[\pi U^2]} + I \tan^{-1}Q/[\pi U^3]} \frac{dU}{dG}. \quad (5)$$

Recall that  $g$  is related to the temperature through

$$g \left( g + \sqrt{g^2 + \frac{\tan^{-1}Q}{\pi U^2}} \right)^{1/3} = Bt, \quad (6)$$

where  $B = (H'_{c2})^2 \xi \phi_0 \sqrt{T_{c0}}/[8\pi\sqrt{2}\kappa^2 k_B]^{2/3}$  and

$$t \equiv \frac{T - T_c(H)}{(HT)^{2/3}}. \quad (7)$$

In the above equations,<sup>25</sup>  $H'_{c2}$  is the first derivative of the critical field  $H_{c2}(T)$  with respect to temperature (and is assumed to be a constant),  $\kappa = \lambda_{ab}/\xi_{ab}$  (where  $\lambda_{ab}$  and  $\xi_{ab}$  are the penetration depth and coherence length respectively in the  $ab$  plane),  $\xi$  is  $\xi_c$  to within a multiplicative constant ( $\xi_c$  is the coherence length along the  $c$  axis),  $T_c(H)$  is the finite field mean-field transition temperature,  $T_{c0} = T_c(0)$ ,  $C_{MF}(T)$

is the mean-field specific heat,  $\phi_0$  is the superconducting flux quantum,  $k_B$  is the Boltzman constant, and  $Q$ ,  $K$ , and  $M$  are adjustable parameters whose values are roughly  $\pi$ ,  $\sqrt{2}$ , and  $2\sqrt{2}$ , respectively. The factor of  $4\pi$  in Eq. (1) is needed to convert  $M(H,T)$  which is in units of emu/cm<sup>3</sup> to gauss (G).

The fits to Eqs. (1) and (2) are nontrivial since  $U(G)$  [Eq. (3)] and  $G(g)$  [Eq. (4)] are functions of one another and the temperature  $T$  is related to  $g$  through a transcendental equation. In place of a commercial fitting package, we have written a code which uses IMSL routines to fit the functions [Eqs. (1) and (2)] (which must be calculated self-consistently) to the data.

The 3D scaling functions [Eqs. (1) and (2)] are more complex than those of the 2D functions because there is an extra length scale which describes the bending of the vortex lines along the field direction (here taken to be the  $c$  axis). For this reason, as we noted above, we will take advantage of the numerical results<sup>22</sup> on the GL-LLL theory for the magnetization, which is the only quantity presently available from numerical work, to ‘‘calibrate’’ certain parameters in our 3D scaling functions.

### B. Magnetization

As explained above, we will begin by narrowing down the number of parameters available to perform fits to actual experimental data by first considering fits to results from a numerical calculation which simulates YBCO. We will then use our results from this fitting as a means of ‘‘calibrating’’ Eqs. (1) and (2).

The numerical calculation to which we refer above was done by Šašik and Stroud<sup>22</sup> using a GL-LLL formulation for a layered system (with parameters similar to those of YBCO  $H'_{c2} = 1.8$  T,  $\kappa = 52$ ,  $T_{c0} = 93$ , and an anisotropy factor  $\gamma = \xi_{ab}/\xi_c = 5$ ) in order to study flux lattice melting. Their results are reproduced in Fig. 1(a). We have done a four-parameter fit of Eq. (1) to this numerical ‘‘data’’<sup>22</sup> and plot our results as lines (solid for 2 T, dashed for 3 T, and dotted for 5 T) with the data in Fig. 1(a). As one can see, the agreement is excellent. The fitting parameters are  $Q$ ,  $K$ ,  $M$ , and the constant  $A$  relating  $\xi$  to  $\xi_c$  and we find  $Q = 10.25$ ,  $K = -5.95$ ,  $M = 7.38$ , and  $\xi = 0.2918\xi_c$  (i.e.,  $A = 0.2918$ ) since  $\xi_c = 2.82$  Å here. To verify the consistency of the numerical data with LLL theory, we scaled the data according to the 3D LLL form  $M(H,T)/(HT)^{2/3} = f[(T - T_c(H))/(TH)^{2/3}]$  and found the data to collapse flawlessly as shown in Fig. 1(b). When doing such scaling, one can typically use  $T_c(H)$  as an adjustable parameter (and, to a lesser extent, the background parameters), but since  $H'_{c2}$  and  $T_{c0}$  are known in this case, there are no adjustable parameters, which makes the scaling of this data very convincing.

Using these values of  $Q$ ,  $K$ ,  $M$ , and  $A$  determined from the fit to the numerical ‘‘data’’ we then performed a fit to the two and three tesla magnetization data of Jeandupeux *et al.*<sup>9</sup> There are nine fitting parameters, namely  $H'_{c2}$ ,  $\kappa$ ,  $\xi_c$ ,  $T_c(2$  T),  $T_c(3$  T),  $B_0(2$  T),  $B_1(2$  T),  $B_0(3$  T), and  $B_1(3$  T) where,  $B_0(H)$  and  $B_1(H)$  are the field-dependent constants used to adjust the subtracted background:  $M_B = (B_0 + B_1/T)H$ .<sup>26</sup> Three-parameter fits were then used to find  $T_c(H)$ ,  $B_0(H)$ , and  $B_1(H)$  for the four and five tesla fields. We find  $\xi_c = 3.78$  Å,  $H'_{c2} = 1.837$  T/K,  $\kappa = 56.02$ , and  $T_c(H) = 90.91$  K, 90.38

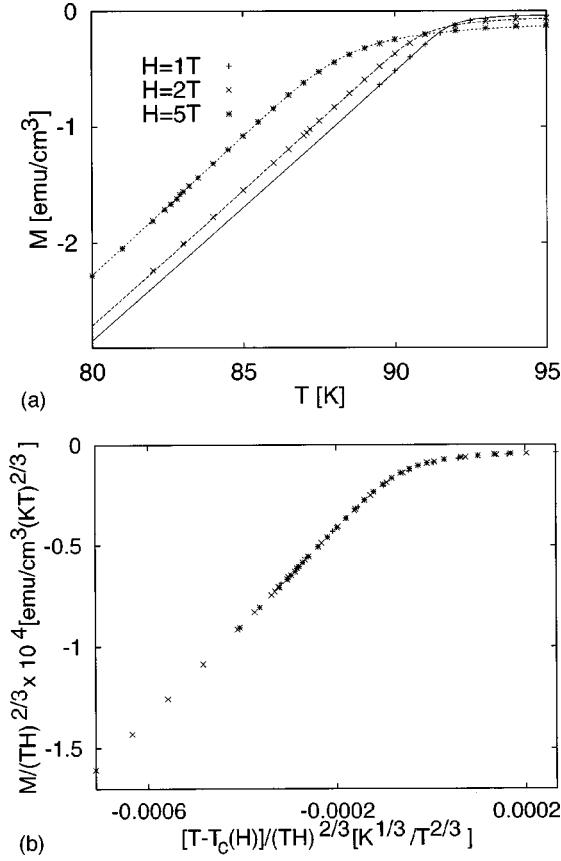


FIG. 1. (a) A fit of Eq. (1) to the “numerical” magnetization data of Ref. 22. (b) The same data (Ref. 22) scaled according to 3D LLL theory.

$K$ ,  $89.83\text{ K}$ , and  $89.04\text{ K}$  for  $H=2\text{ T}$ ,  $3\text{ T}$ ,  $4\text{ T}$ , and  $5\text{ T}$ , respectively and show the fits in Fig. 2. The fit to the  $5\text{ T}$  data is the least satisfactory which we attribute to the data: One can see from Fig. 3 of Ref. 9 that the  $4\text{ T}$  and  $5\text{ T}$  data have spurious behavior at low temperatures instead of collapsing to the mean-field temperature dependence which could be a result of the entry into the irreversible region. Except for the  $5\text{ T}$  fit, the fits are reasonable and the parameter values are similar to those found by others which gives us confidence that the theory is a good description of the data. Furthermore, when one compares the value of  $H'_{c2}$  obtained in the fits to the values  $H'_{c2}=1.85\text{ T/K}$  found from the  $T_c(H)$ 's for  $H=2-4\text{ T}$  (throwing out the less satisfactory  $5\text{ T}$  fit), one finds good agreement strengthening the credibility of the fit. If the quantities  $Q$ ,  $K$ , and  $M$  are added as fitting parameters, rather than being taken as obtained from the numerical “calibration,” significantly better fits are not obtained. This is as expected, if the procedure is correct.

In the inset to Fig. 2, we show the LLL scaling of the magnetization data of Ref. 9 using the parameters obtained from our fit. The collapse of the data is good in the critical region but fans out somewhat in the low-temperature, mean field region. We believe that some of this fanning may be due to the spurious behavior associated with the irreversible region which we discussed above.<sup>27</sup>

We have also attempted fits to the magnetization data on a YBCO single crystal by Salem-Sugui and da Silva.<sup>28</sup> In this case the fits were rather poor unless unphysical parameter

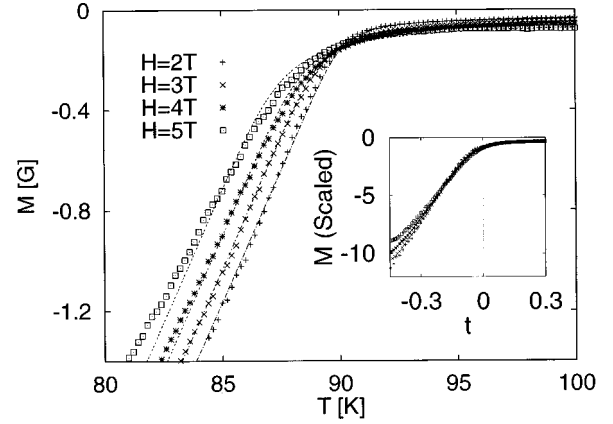


FIG. 2. The magnetization data from a YBCO twinned single crystal published in Ref. 9 along with the fits to Eq. (1). (Inset: Our LLL scaling of the magnetization data of Ref. 9 shown over a larger range than that of the authors of Ref. 9 which is in the inset to Fig. 5 of that reference. The y axis is  $4\pi M/(TH)^{2/3} \times 10^4$   $[\text{G}/(\text{OeK})^{2/3}]$  and the x axis is  $t \times 10^3$   $[\text{K}^{1/3}/\text{Oe}^{2/3}]$  where  $t$  is defined in Eq. (7).)

values were chosen. The situation did not improve when  $Q$ ,  $K$ , and  $M$  were added as fitting parameters. This is in contradistinction with what occurs with the numerical results and with the data of Ref. 9. We are more inclined to believe that the origin of the discrepancy lies with the data set than with the theory, but we cannot be certain until more magnetization data from YBCO becomes available to us.

We now turn to using Eq. (1) to explain the results of Ref. 23 in which it was found that the temperature derivative of the magnetization has an approximately field independent value and a crossover point at a distinct temperature whose value lies close to that of  $T_{c0}$  for YBCO.

### C. Behavior of the magnetization temperature derivative

The behavior of the temperature derivative of the magnetization  $\partial M(H, T)/\partial T$  has been studied as a function of the field  $H$  in Ref. 23. The behavior is quite striking. The most salient feature of the experimental results (Fig. 2 of Ref. 23) is the very weak dependence on the field of this partial derivative at temperatures near the mean-field temperature. This weak dependence extends to a rather wide temperature range (more than eight degrees) and in fact, can nearly be called a field independence for the fields  $H \geq 2$  for both the YBCO and BSCCO data. Also remarkable is the feature upon which the authors in the cited experimental work focused which is the apparent crossing of the data at a temperature very close to  $T_{c0}$ .

These experimental results can be easily understood from the LLL scaling formula, Eq. (1). This equation can be rewritten simply as

$$M = (HT)^{2/3} \mu(t), \quad (8)$$

where  $\mu$  is the scaling function and  $t$  the scaled temperature variable defined in Eq. (7). From these equations we have for the temperature derivative

$$\frac{\partial M}{\partial T} = \frac{2}{3} (HT)^{-1/3} \mu(t) + \mu'(t) \left( 1 - \frac{2}{3} \frac{T - T_c(H)}{T} \right), \quad (9)$$

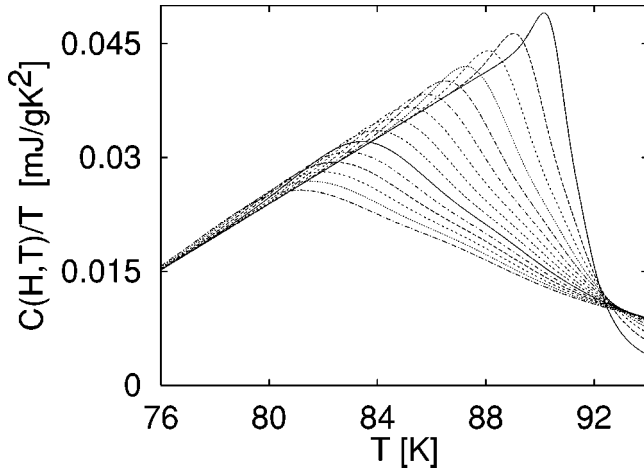


FIG. 3. Theoretical specific heat curves for various fields ( $H=1-8$  T plotted at 0.5 T intervals) calculated from Eq. (2).

where  $\mu'(t)$  is the derivative of  $\mu(t)$  with respect to its argument. We can proceed to the evaluation of the mixed second partial derivative, with the result

$$\begin{aligned} \frac{\partial^2 M}{\partial T \partial H} &= \frac{4}{9} \frac{1}{HT} (\mu(t)(HT)^{2/3} - \mu'(t)[T - T_c(H)]) - \mu''(t) \\ &\times \left( 1 - \frac{2}{3} \frac{T - T_c(H)}{T} \right) \frac{1}{HT^{2/3}} \left( \frac{1}{H'_{c2}} + \frac{2}{3} \frac{T - T_c(H)}{H} \right), \end{aligned} \quad (10)$$

where we have used  $dT_c(H)/dH = 1/H'_{c2}$ . Because the scaling function for the magnetization is essentially a linear function of its argument (except in a very narrow region near its kink), we can drop the term proportional to  $\mu''$  in Eq. (10). We then have that the condition for the mixed derivative to vanish is

$$(HT)^{-1/3} \mu(t) = \mu'(t) \frac{T - T_c(H)}{HT}, \quad (11)$$

which, taking into account Eq. (7), can be written

$$\mu(t) = \mu'(t)t \approx \mu'(0)t. \quad (12)$$

Since  $\mu(0)$  is small, this relation is to good accuracy the Taylor expansion of  $\mu(t)$  about  $t=0$  and it will trivially hold over an extended region. Indeed, since  $\mu$  is nearly everywhere linear, so that there are no higher order terms, it may appear that we have nearly proved that the vanishing of the mixed derivative is an identity. This is not at all the case, chiefly because  $\mu(0)$  cannot everywhere be neglected. However, the argument makes it abundantly clear that the weak dependence on the field of the mixed derivative of  $M$  and the crossing point follow easily from LLL scaling.

#### D. Specific heat

In this section we will examine the specific heat function [Eq. (2)] fitting the data of Ref. 9 to it. We will then use Eq. (2) and the method of Ref. 29 to show that flux lattice melting occurs at about the same temperature as the onset of  $H_{c2}$  (or LLL) fluctuations.

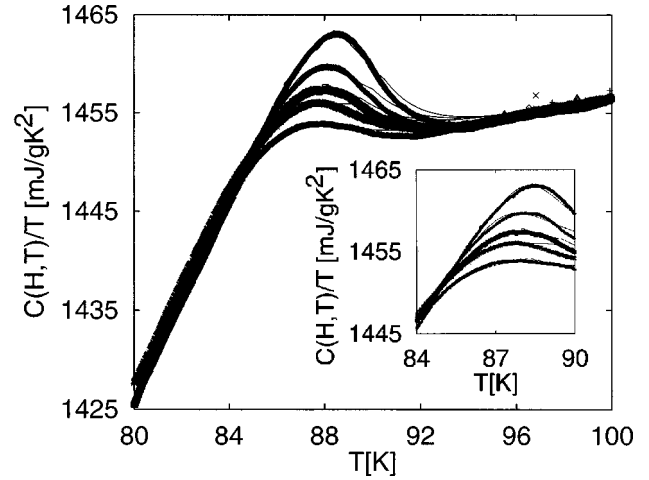


FIG. 4. YBCO specific heat data for various fields ( $H=3,4,5,6,7$  T) from Ref. 9 along with the fits to Eq. (2). The uppermost curve corresponds to  $H=3$  T, and the lowermost curve to  $H=7$  T. (Inset: The same figure zoomed in to show the critical region.)

We begin by examining the specific heat curves produced by Eq. (2). We display this function divided by temperature in Fig. 3 for various fields in the vicinity of the critical area using parameters characteristic of YBCO and units of  $\text{mJ/gK}^2$ . (For YBCO,  $1.0 \text{ mJ/gK} = 0.6698 \text{ J/mole K}$ .) For  $C_{\text{MF}}(T)$ , we used a standard form:  $C_{\text{MF}}(T) = \gamma T [1 + b(T/T_{c0} - 1)]$  which was taken to be a constant above  $T_c(H)$ . This form produces an artificial nonanalyticity of the curves at  $T_c(H)$  since the first derivatives are not continuous but this is unimportant since it does not affect our analysis in any significant way. As one can see in Fig. 3, the curves generated from Eq. (2), which have the features of a mean-field ‘‘ramp’’ with fluctuations which produce a peak, are qualitatively similar to the data from YBCO samples. See, for example, Fig. 2 of Ref. 9 (reproduced here in Fig. 4), Fig. 1 of Ref. 29, or Fig. 2 of Ref. 7. What is common to all of these curves is that they do not collapse immediately for temperatures below the peak. This is in agreement with a result derived from LLL theory, as originally pointed out in Ref. 22. There, using the Maxwell relation,  $(\partial^2 M / \partial T^2)_H = (\partial C_H / \partial H)_T / T$ , it was noted that the left hand side of this equation is positive for lower temperatures, which means that  $C(T, H)$  must increase with increasing field.<sup>30</sup> As we will discuss below (Sec. II E), 3D XY theory cannot account for such behavior.

We have attempted fits of the specific heat data of Ref. 9 to Eq. (2). The best test of the theory would be to be able to fit the specific heat data with the parameters obtained for the magnetization data on the same sample, which was discussed in Sec. II B. This could not be done however, and a good fit to the entire relevant temperature range could not be obtained even when lifting the constraints from the magnetization fits. In our opinion this is due in part to the approximations used to obtain Eq. (2), and in part to the 3D specific heat function *above the peaks* not having the same qualitative behavior as data from YBCO samples which we believe exhibits 2D behavior in this region. The experimental side of the latter statement is reasonable since 2D fluctuations have been observed in these materials through electronic transport

measurements.<sup>31</sup> (For evidence in specific heat data, see Refs. 6,7.) The theoretical side of these statements is plausible for the following reasons. First, as one can see, the theoretical curves for three dimensions exhibit a crossover point above the peak which according to the Maxwell relation  $(\partial^2 M / \partial T^2)_H = (\partial C_H / \partial H)_T / T$  would lead to a positive curvature in the magnetization for temperatures above the crossover point. This is not observed in YBCO materials. This inconsistency must be attributed to the approximation used to obtain the specific heat function as a derivative of the free energy, which worsens in the region above  $T_c(H)$ . (The magnetization function involves fewer approximations.<sup>11</sup>) Secondly, the 2D curves decay more quickly to zero above the transition than the 3D curves which is important as we now show.

To account for the apparent dimensional crossover of the specific heat data, we have done fits of the 2D function<sup>11</sup> to the data omitting a sizeable temperature window [83.3 K:91.5 K] around the peak where the 3D behavior is expected to dominate in order to fix the background [ $C_B = (-8.6336 + 2.2602 T) \text{ mJ/gK}$ ]. We then do a fit of the 3D function to the 3 T, 4 T, 5 T, 6 T, and 7 T specific heat data for the temperature range [82 K:89 K]. The results are good as can be seen from the parameter values:  $H'_{c2} = 1.82 \text{ T/K}$ ,  $\kappa = 65.6$ , and  $\xi_c = 3.1819$ . This is reinforced by a visual inspection of the fit in Fig. 4 where the curves agree quite well in the region we believe to be 3D. One also notices that the curves are on the high side at temperatures above the peak, which agrees with our earlier discussion of this temperature regime.

The parameter space is large here and it would be impossible to explore all of it to determine the very best fit. From our investigations however, we are certain that an improved fit with better parameter values can be obtained for example by allowing  $Q$ ,  $K$ , and  $M$  to vary. One could also allow for a quadratic term in the background or even in the mean-field term which we have extended over a large temperature range. Even without exploring the large parameter space, we have demonstrated the agreement between the 3D LLL specific heat function [Eq. (2)] and YBCO data.

In the remainder of this subsection, we will discuss more indirect consequences of LLL theory as applied to the specific heat of YBCO class materials. We will present evidence, using Eq. (2) and the method of Ref. 29, that flux lattice melting, which has been observed in resistivity and magnetization measurements<sup>32</sup> and more recently in high quality calorimetric and specific heat measurements,<sup>29,33-35</sup> coincides with the onset of LLL fluctuations.<sup>19,20</sup> As we pointed out above, the curves in Fig. 3 produced from Eq. (2) reproduce the key features of specific heat data from YBCO samples, such as that seen in Fig. 1 of Ref. 29, especially for temperatures below the peak. As the field increases, the peak in the theoretical curves moves down in temperature and broadens. Similarly, the temperature of the onset of the fluctuation part of the peak moves down. By considering the behavior of this temperature as a function of field with flux lattice melting lines obtained from Ref. 29 and elsewhere,<sup>32</sup> we will now demonstrate the stated correspondence.

To arrive at their conclusion of second-order flux lattice melting Roulin, Junod, and Walker<sup>29</sup> subtract a data set for one field from a data set from a slightly larger field and find

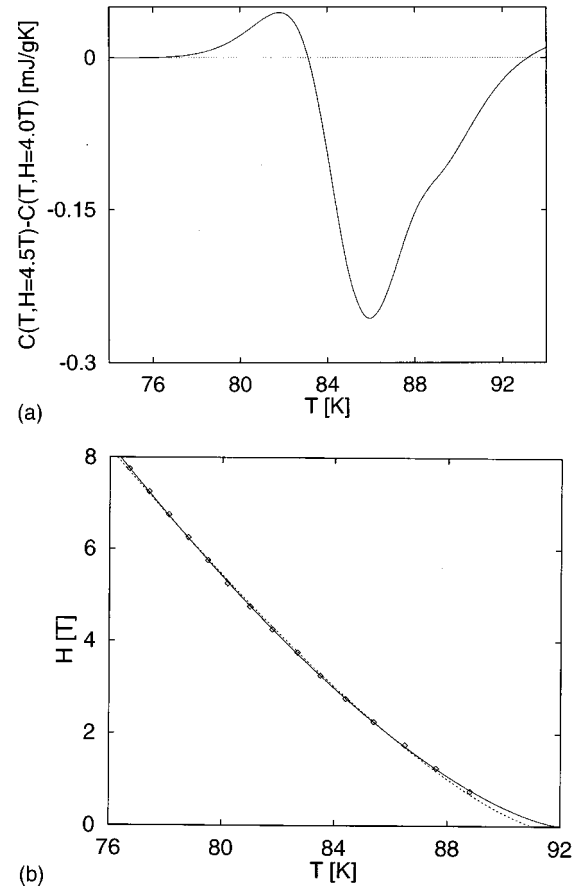


FIG. 5. (a)  $\delta C(T, H=4.25 \text{ T}) = C(T, H=4.5 \text{ T}) - C(T, H=4.0 \text{ T})$  (a “differential”) determined from two of the theoretical curves in Fig. 3. This curve has the same qualitative behavior as Fig. 2(b) of Ref. 29. (b) The field value versus the temperature at which the “differentials” peak (as explained in the text) for those fields and two theoretical fits which are discussed in Secs. II D and II E.

a peak in the “differential.” This peak is due to the higher field starting to peak at a slightly lower temperature due to peak broadening and transition temperature suppression. To see if this peak corresponds to a flux lattice melting, they look at the field dependence of the peak temperature and find that it agrees with the same curve found in Ref. 32 by analysis of magnetization and resistivity curves to derive a flux lattice melting line for a YBCO sample. We will now show that similar results can be obtained from Eq. (2).

Consider Fig. 5(a). Here,  $\delta C(T, H=4.25 \text{ T}) \equiv C(T, H=4.5 \text{ T}) - C(T, H=4.0 \text{ T})$ , the difference of two theoretical curves calculated from Eq. (2), is plotted and is seen to have the same behavior as that of Fig. 2(b) in Ref. 29: a peak followed by a deep trough. The field dependence of the temperature at which each  $\delta C(T, H)$  peaks is then calculated. This is plotted in Fig. 5(b) along with two lines. The first line (solid line) is the best three parameter fit of this theoretical LLL result to the function  $H(T) = a(1 - T/b)^c$  with  $a = 111.2$ ,  $b = 92.1$ , and  $c = 1.48$  (standard deviation = 0.02). The second (dashed) line is a two parameter fit with a fixed  $c = 1.33$  and  $a = 89.2$  and  $b = 91.1$  (standard deviation = 0.05). One can see that while the exponents differ by 11%, the two curves are hard to distinguish. These lines are to be contrasted to that of Refs. 29,32 where the correspond-

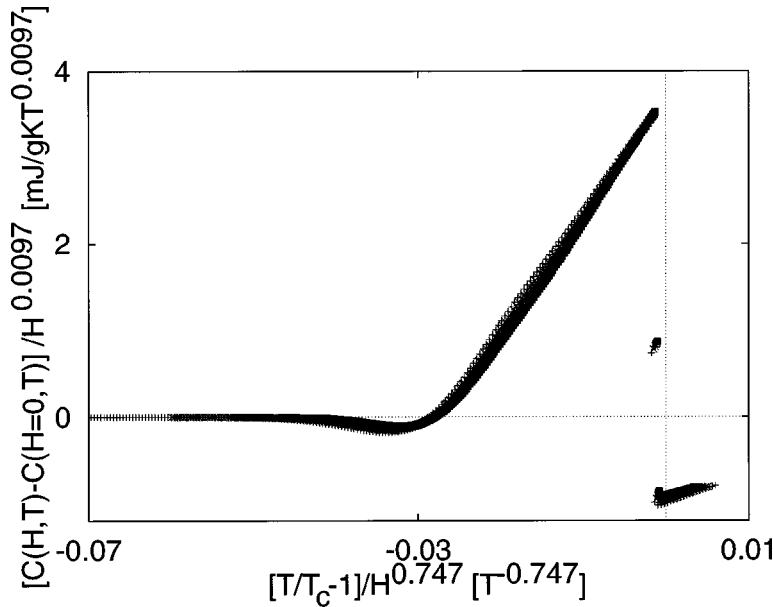


FIG. 6. The theoretical specific heat curves from an LLL calculated Eq. (2) (Fig. 3) scaled according to 3D XY theory: Eq. (13).

ing line,  $H_m(T) = 99.7[1 - T/92.5]^{1.36}$ , is identified with the second order melting line. The numbers in both fits agree quite well with each other, especially the exponent which is the most critical parameter in this curve. However, in our case it has no direct relation to the melting. It therefore seems that the onset of LLL fluctuations coincides with flux lattice melting. Further evidence of this has been provided in Refs. 19,20. The melting line is predicted<sup>19</sup> to be where Eq. (7) is a constant and it has been shown<sup>20</sup> that this is consistent with the melting lines found above.

### E. Implications for 3D XY scaling

In this subsection, we will address an important question concerning the experimental discrimination between LLL and 3D XY scaling. We will show that the LLL theoretical results derived from Eqs. (1) and (2) can be used to generate curves which can then apparently be scaled in accordance with 3D XY theory. Thus, finding 3D XY scaling does not exclude that the data actually is in agreement with GL-LLL theory. Further, the importance of comparing the experimental results with computed functions, not now available for 3D XY theory, is made obvious.

There are two procedures that have been used to analyze specific heat data according to 3D XY scaling theory. The first is that derived in Ref. 36:

$$\frac{C(H,T) - C(H=0,T)}{H^{0.0097}} = f\left(\frac{T/T_c - 1}{H^{0.747}}\right), \quad (13)$$

where  $T_c$  is the zero-field critical temperature and the second is that derived in Ref. 1:

$$\frac{C_{SC}(H,T) - C_0}{H^{0.0097}} = f\left(\frac{T/T_c - 1}{H^{0.747}}\right), \quad (14)$$

where  $C_0$  is the height of the specific heat cusp and the subscript SC signifies that it is only the superconducting contribution, with the background subtracted out. [The exponent for  $H$  on the right hand side (RHS) of these equations is derived from the specific heat exponent  $\alpha$  and we have used

the value derived from <sup>4</sup>He experiments. The theoretical value of  $\alpha$  is 0.005.] The second scaling form<sup>1</sup> is the more convincing one since the scaling takes place over a wider and less trivial range. In the first form on the other hand, one is scaling mostly horizontal lines which are equal to zero,<sup>36</sup> and thus are virtually guaranteed to scale. The first form thereby acts as a sufficient condition for 3D XY scaling and we use it here. If it does not scale according to this form, it certainly will not scale according to Eq. (14).

Thus, we proceed to generate “data” from the theoretical expression Eq. (2). This is a portion of the theoretical results shown earlier in Fig. 3. Then, we attempt to scale this “data” according to the 3D XY formula. The scaling results are shown in Fig. 6 for the 4 T, 5 T, 6 T, 7 T, and 8 T fields and as one can see, the collapse is reasonable. We have left out the smaller fields which as one would expect do not collapse onto these curves. If one were to consider the noise, and the background subtractions, which inevitably enter into the analysis of actual experimental data, one could call our scaling convincing. [When the exponent 0.005 is used for the exponent for  $H$  on the RHS of Eq. (13), the “data” does not collapse quite as well.] That LLL calculated “data” can be made to scale according to 3D XY theory exemplifies the excessive generality of mere scaling and reinforces the statement made in the Introduction that apparently good agreement scaling is not sufficient to prove the validity of a theory. This was also stated in Ref. 9 within the context of the 3D XY theory.

As a further insight on these problems, we comment on actual specific heat data from a YBCO sample which was scaled using Eq. (13) the same way as the theoretical curves in Fig. 6. This is the specific heat data of Ref. 9, the same data to which we attempted fits in Sec. II D. The 3D XY scaling results in that work are shown in Fig. 4 in Ref. 9. The large central peak is the zero-field peak and so of course it is unimportant since it is simply an artifact of having subtracted off the zero-field data. The important region to consider is just to the left of the central peak, since that area represents the peaks (or the region of critical behavior) of the finite-field data sets. As one can see, the data is not close to col-

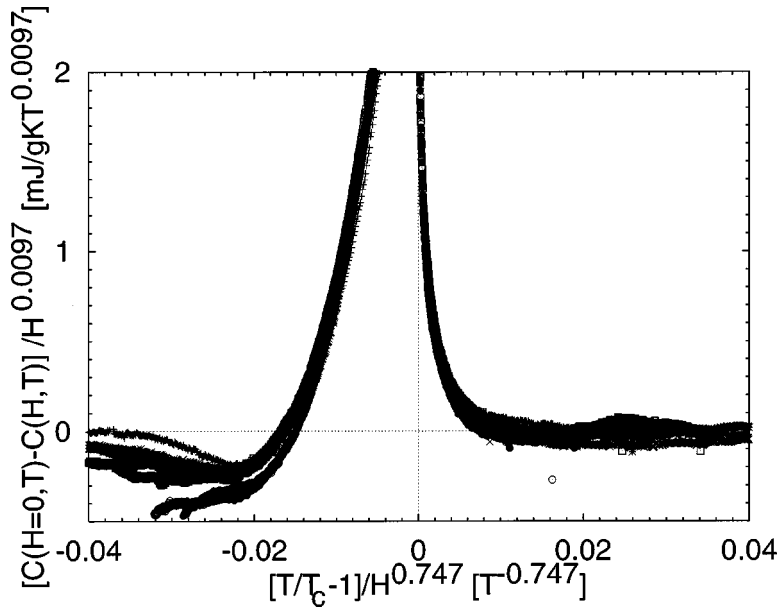


FIG. 7. The data of Ref. 9 scaled according to 3D XY theory. The critical region is to the left of the large peak which is the zero-field peak. One can see that 3D XY scaling does not describe the critical region. There are seven data sets plotted, corresponding to fields of 1 to 7 T at 1 T intervals. Higher field sets have lower values at the extreme left of the graph.

lapsing here. Because this data is plotted on a scale which brings in the size of the irrelevant, large zero-field peak, scaling does not appear to be a dramatic failure. However when compared to the collapse of the data at temperatures above the peak where there are no fluctuations and one is dealing with only the background, one can see that the failure of 3D XY scaling is more obvious. We have done our own similar analysis on this data which we show in Fig. 7 in a more restricted scale. [We emphasize the point that if the data does not scale with Eq. (13), it will not scale with the more convincing Eq. (14).] It is seen that the 2 T and 3 T data do collapse but the 1 T data rides high and the larger fields go low. The failure of the scaled data to collapse in the actual critical region makes one question whether 3D XY behavior is valid, although it does not rule it out. Derivations of the actual functions like those of Ref. 10 would allow us to settle the point. This is why such derivations are so important.

We close this section on implications for 3D XY scaling with a discussion of the references to 3D XY in the flux lattice melting literature. There a melting line of the form  $H_m(T) = 99.7[1 - T/T_c(0)]^{1.36}$  is found by many authors<sup>29,32,37</sup> who point out that the exponent here is the nearly the same as that (1.33) expected for 3D XY critical point analysis. And while some of the same authors<sup>32</sup> note that such an analysis appears incompatible with a first-order transition, that we get the same exponent from a LLL approach appears to make such an identification with 3D XY theory even more unlikely.

### III. DISCUSSION AND SUMMARY

In this paper, we have studied the relevance of 3D GL-LLL theory as exemplified by Eqs. (1) and (2) for the magnetization and specific heat, to the relatively isotropic HTSC materials of the YBCO family.

Equation (1) was found to accurately describe the magnetization data for a YBCO sample<sup>9</sup> and the numerical data modeling these materials in the GL-LLL formalism.<sup>22</sup> In the former case, several of the fitting parameters were obtained

independently from fits to the numerical calculation thereby raising the credibility of the fits. The remaining parameter values ( $H'_{c2}$ ,  $\kappa$ , and  $\xi_c$ ) correspond well to those found for these materials by other means. When applied to another data set,<sup>28</sup> Eq. (1) was not found to accurately describe it. We obviously cannot completely rule out that the results in the last reference are the correct ones and that the other two are wrong, but it seems unlikely to us. We also found that Eq. (2) could not describe the YBCO specific heat data of Ref. 9 over the whole temperature [80 K:100 K] but that very good results for five of the fields could be obtained if the region above the peak is excluded from the fit. The question of why this is brings us now to a broader discussion of the applicability of both the 3D specific and magnetization functions of Ref. 11 to YBCO data.

As we discussed in the Introduction, several factors could explain possible discrepancies between the functions and the data. The most significant would be the failure of GL-LLL theory to describe the YBCO data. We believe that the evidence is against this because it has been shown elsewhere (as mentioned in the Introduction) that YBCO data scales according to this theory. Another possible reason would be discrepancies between the functions of Ref. 11 and exact GL-LLL theory. While it does seem that there are some problems with the approximations used to obtain Eq. (2) for temperatures above the peak, we tend to discount this for temperatures around and below the specific heat peaks for two reasons. First, the 2D function was found to have significant success in describing the more anisotropic HTSC materials and is known to be in excellent agreement with numerical simulations of the 2D GL-LLL theory. Secondly, we note the exceptional fit of Eq. (1) to the numerical data [Fig. 1(a)] which provides evidence that this equation is an accurate description of the GL-LLL theory.

Part of the shortcomings also arise, we believe, because Eqs. (1) and (2) are 3D functions and it has been shown that, while the YBCO is the least anisotropic of the major HTSC materials, 2D signatures are present.<sup>31</sup> As mentioned above, we have tested this by successfully fitting the 3D LLL function to the temperature range of the specific



heat data which is believed to be 3D. Further adding to our conclusion here is prior evidence for 2D behavior in YBCO and LBCO through specific heat LLL scaling.<sup>6,7</sup> The problems that afflict the specific heat do not affect the magnetization, which has a much simpler, monotonic behavior. To try to remedy the specific heat problem by splicing together the 2D and 3D functions in the appropriate temperature ranges to describe the YBCO data would introduce so many fitting parameters that any fit would be of little value. It is also possible to use the quasi-2D functions of Ref. 11 but these also have a large number of fitting parameters besides being much less tractable than the pure 2D or 3D functions.

The importance of scaling functions, as contrasted to mere scaling variables, has been demonstrated in this paper by showing the low information content of 3D  $XY$  scaling without the associated scaling functions. It was shown in two cases (Sec. II E) how curves from an equation calculated using LLL assumptions could be described by 3D  $XY$  theory.

This has consequential ramifications for the significance of 3D  $XY$  theory and what it means to find that data scales according to 3D  $XY$  theory. Knowledge of the expressions for the 3D  $XY$  scaling functions would be very desirable. If such a calculation becomes available, it would be very worthwhile to repeat the analysis done in this paper in terms of such functions.

## ACKNOWLEDGMENTS

Conversations with Dr. J. Buan and Professor C. C. Huang are gratefully acknowledged as is a fruitful discussion with Dr. A. Junod. We thank Dr. Šášík, and Dr. Stroud, Dr. Salem-Sugui Jr. *et al.*, and Dr. O. Jeandupeux *et al.* for generously providing their data. We also thank Isaac Rutel for assistance with the data used in Figs. 6 and 7. This work has been supported in part by the NSF Grant No. DMR-9415549.

\*Electronic address: pierson@wpi.edu.

- <sup>1</sup>N. Overend, M. A. Howson, and I. D. Lawrie, *Phys. Rev. Lett.* **72**, 3238 (1994).
- <sup>2</sup>S. W. Pierson, J. Buan, B. Zhou, C. C. Huang, and O. T. Valls, *Phys. Rev. Lett.* **74**, 1887 (1995).
- <sup>3</sup>M. Roulin, A. Junod, and J. Muller, *Phys. Rev. Lett.* **75**, 1869 (1995).
- <sup>4</sup>A. Junod, M. Roulin, and E. Walker, *Physica C* **260**, 257 (1996).
- <sup>5</sup>K. Moloni, M. Friesen, S. Li, V. Souw, P. Metcalf, L. Hou, and M. McElfresh, *Phys. Rev. Lett.* **78**, 3173 (1997).
- <sup>6</sup>S. W. Pierson, T. M. Katona, Z. Tešanović, and O. T. Valls, *Phys. Rev. B* **53**, 8638 (1996).
- <sup>7</sup>B. Zhou, J. Buan, S. W. Pierson, C. C. Huang, O. T. Valls, J. Z. Liu, and R. N. Shelton, *Phys. Rev. B* **47**, 11 631 (1993).
- <sup>8</sup>N. Overend, M. A. Howson, I. D. Lawrie, S. Abell, P. J. Hirst, C. Changkang, S. Chowdhury, J. W. Hodby, S. E. Inderhees, and M. B. Salamon, *Phys. Rev. B* **54**, 9499 (1996).
- <sup>9</sup>O. Jeandupeux, A. Schilling, H. R. Ott, and A. van Otterlo, *Phys. Rev. B* **53**, 12 475 (1996).
- <sup>10</sup>Z. Tešanović, L. Xing, L. N. Bulaevskii, Q. Li, and M. Suenaga, *Phys. Rev. Lett.* **69**, 3563 (1992).
- <sup>11</sup>Z. Tešanović and A. V. Andreev, *Phys. Rev. B* **49**, 4064 (1994).
- <sup>12</sup>L. N. Bulaevskii, M. Ledvij, and V. G. Kogan, *Phys. Rev. Lett.* **68**, 3773 (1992).
- <sup>13</sup>See, for example, P. H. Kes, C. J. van der Beek, M. P. Maley, M. E. McHenry, D. A. Huse, M. J. V. Menken, and A. A. Menkovsky, *Phys. Rev. Lett.* **67**, 2383 (1991); R. Jin, A. Schilling, and H. R. Ott, *Phys. Rev. B* **49**, 9218 (1994); Q. Li, M. Suenaga, G. D. Gu, and N. Koshizuka, *ibid.* **50**, 6489 (1994).
- <sup>14</sup>A. Wahl, A. Maignan, C. Martin, V. Hardy, J. Provost, and Ch. Simon, *Phys. Rev. B* **51**, 9123 (1995).
- <sup>15</sup>N. Kobayashi, K. Egawa, K. Miyoshi, H. Iwasaki, H. Ikeda, and R. Yoshizaki, *Physica C* **219**, 265 (1994).
- <sup>16</sup>See also, A. Carrington, A. P. Mackenzie, and A. Tyler, *Phys. Rev. B* **54**, R3788 (1996); A. Carrington, C. Marcenat, F. Bouquet, D. Colson, and V. Viallet, *Czech. J. Phys.* **46**, Suppl. 6, 3177 (1996).
- <sup>17</sup>M. Roulin, A. Junod, E. Walker, and A. Erb, *Physica C* **282-287**, 1401 (1997).
- <sup>18</sup>It should be noted that in the equation for the 3D specific heat function [Eq. (27)] in Ref. 11, only leading terms were included.

In general, the subleading terms are needed to reproduce the peak in the 3D LLL specific heat function. Such terms can be extracted from the 3D limit of the general expression [Eq. (30)] in Ref. 11.

- <sup>19</sup>I. F. Herbut and Z. Tešanović, *Physica C* **225**, 324 (1995).
- <sup>20</sup>S. W. Pierson and O. T. Valls (unpublished).
- <sup>21</sup>See Ref. 11 and also J. Hu and A. H. MacDonald, *Phys. Rev. B* **52**, 1286 (1995); J. Hu, Ph.D. thesis, Indiana University, 1994.
- <sup>22</sup>R. Šášík and D. Stroud, *Phys. Rev. Lett.* **75**, 2582 (1995).
- <sup>23</sup>O. Jeandupeux, B. Heeb, and H. R. Ott, *Physica C* **264**, 191 (1996).
- <sup>24</sup>The resulting expression is more accurate than that quoted for the pure 3D limit in Ref. 11 which includes leading terms only.
- <sup>25</sup>We have used the following Ginzburg-Landau (GL) isotropic relations in going from Eqs. (24) and (26) of Ref. 11 to Eqs. (1) and (2):  $\gamma = \hbar^2/2m^* = \alpha' \xi^2 T_{c0}$ , and  $\alpha'^2/\beta = C_M F(T)/T = H'_{c2}{}^2/[8\pi\kappa^2]$  where  $\alpha$ ,  $\beta$ , and  $\gamma$  are the GL parameters and  $\alpha' = d\alpha/dT$  evaluated at  $T_{c0}$ . See M. Tinkham, *Introduction to Superconductivity* (McGraw-Hill, New York, 1996), Chap. 4.
- <sup>26</sup>The data were made available to us with a background term already subtracted in connection with a different fitting; the subtraction discussed here refers therefore to an adjustment in the background term.
- <sup>27</sup>It should be noted that our 3D LLL scaling of this data is an improvement of that done on this data by the authors of Ref. 9 which is shown in their inset to Fig. 5 over a more restricted scale.
- <sup>28</sup>E. Z. da Silva and S. Salem-Sugui, Jr., *Physica C* **257**, 173 (1996); **235-240**, 1919 (1994).
- <sup>29</sup>M. Roulin, A. Junod, and E. Walker, *Science* **273**, 1210 (1996).
- <sup>30</sup>At temperatures just below the transition temperature, it was observed by the authors of Ref. 22 that  $(\partial^2 M/\partial T^2)_H$  is negative implying that  $(\partial C_H/\partial H)_T$  must also be negative as observed in Fig. 3. This region corresponds to the vortex liquid phase and when  $(\partial^2 M/\partial T^2)_H$  is positive, the region is a vortex solid phase. This is consistent with the idea presented here and elsewhere (Refs. 19 and 20) that the onset of  $H_{c2}$  or LLL fluctuations coincides with flux lattice melting except that this theory predicts that the flux lattice melting will occur within the region where  $(\partial^2 M/\partial T^2)_H > 0$ .

- <sup>31</sup>See, for example, N.-C. Yeh and C. C. Tsuei, *Phys. Rev. B* **39**, 9708 (1989); Q. Y. Ying and H. S. Kwok, *ibid.* **42**, 2242 (1990); P. C. E. Stamp, L. Forro, and C. Ayache, *ibid.* **38**, 2847 (1988); T. M. Katona and S. W. Pierson, *Physica C* **270**, 242 (1996); P. Minnhagen and P. Olsson, *Phys. Rev. Lett.* **67**, 1039 (1991); V. Persico, V. Cataudella, F. Fontana, and P. Minnhagen, *Physica C* **260**, 41 (1996).
- <sup>32</sup>U. Welp, J. A. Fendrich, W. K. Kwok, G. W. Crabtree, and B. W. Veal, *Phys. Rev. Lett.* **76**, 4809 (1996).
- <sup>33</sup>M. Roulin, A. Junod, A. Erb, and E. Walker, *J. Low Temp. Phys.* **105**, 1099 (1996).
- <sup>34</sup>A. Schilling, R. A. Fisher, N. E. Phillips, U. Welp, W. K. Kwok, and G. W. Crabtree, *Phys. Rev. Lett.* **78**, 4833 (1997).
- <sup>35</sup>See also A. Schilling, R. A. Fisher, N. E. Phillips, U. Welp, D. Dasgupta, W. K. Kwok, and G. W. Crabtree, *Nature (London)* **382**, 791 (1996), and references therein.
- <sup>36</sup>M. B. Salamon, J. Shi, N. Overend, and M. A. Howson, *Phys. Rev. B* **47**, 5520 (1993).
- <sup>37</sup>R. Liang, D. A. Bonn, and W. N. Hardy, *Phys. Rev. Lett.* **76**, 835 (1996).